

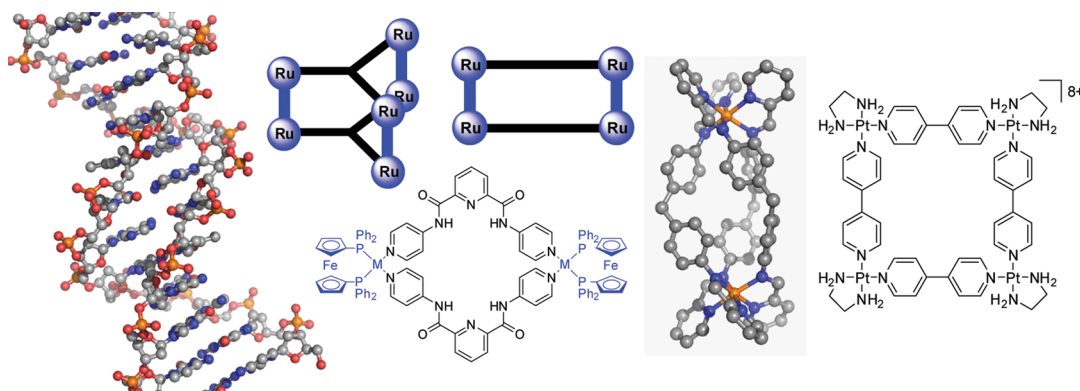
Biomedical and Biochemical Applications of Self-Assembled Metallacycles and Metallacages

TIMOTHY R. COOK,^{†,*} VAISHALI VAJPAYEE,[‡] MIN HYUNG LEE,[‡]
PETER J. STANG,^{†,*} AND KI-WHAN CHI^{‡,*}

[†]*Department of Chemistry, University of Utah, 315 South 1400 East,
Salt Lake City, Utah 84112, United States, and* [‡]*Department of Chemistry,
University of Ulsan, Ulsan 680-749, Republic of Korea*

RECEIVED ON JANUARY 15, 2013

CONSPECTUS



Metal ions and metal complexes with organic molecules are ubiquitous in nature. Bulk metal ions of Na, K, Mg, and Ca constitute as much as 1% of human body weight. The remaining trace ions, most commonly of Fe, Ni, Cu, Mn, Zn, Co, Mo, and V, make up ~0.01% by weight, but their importance in biological processes cannot be overstated.

Although nature is limited to the use of bioavailable metal ions, many rarer transition metals can elicit novel biological responses when they interact with biomolecules. For this reason, metal–biomolecule complexes are of interest in medicinal applications. A well-known example is cisplatin, which contains Pt, rare in nature, but highly effective in this context as an anticancer drug in the form of *cis*-Pt(NH₃)₂Cl₂ and analogous Pt(II) complexes. This and other examples have led to strong interest in discovering new metalloanticancer drugs.

In this Account, we describe recent developments in this area, particularly, using coordination-driven self-assembly to form tunable supramolecular coordination complexes (SCCs) with biomedical applications. Coordination-driven self-assembly describes the spontaneous formation of metal–ligand bonds in solution, transforming molecular building blocks into single, 2D metallacycles, or 3D metallacages depending on the directionality of the precursors used. Such SCCs have well-defined internal cavities and simple pre- or post-self-assembly functionalizations. They are highly tunable both spatially and electronically.

Metal ions are necessary structural elements for the directional bonding approach, which can be exploited to provide biological activity to an SCC, particularly for Pt- and Ru-based structures. Since these two metals are not only among the most commonly used for coordination-driven self-assembly but are also the basis for a number of small molecule anticancer agents, researchers have evaluated a growing number of SCCs for their antitumor properties.

The biological application of SCCs is still an emergent field of study, but the examples discussed in this Account confirm that supramolecular scaffolds have relevance to a wide variety of biochemical and biomedical targets. SCCs can serve as anticancer agents, act as selective sensors for biologically important analytes, or interact with DNA and proteins. The myriad of possible SCCs and their almost limitless modularity and tunability without significant synthetic penalty suggests that the biological applications of such species will continue along this already promising path.

Introduction

The use of synthetic coordination complexes in biological settings is a logical extension of the studies of natural

systems which reveal that, despite a common association of biochemistry with organic molecules and transformations, metal ions and complexes are found ubiquitously.

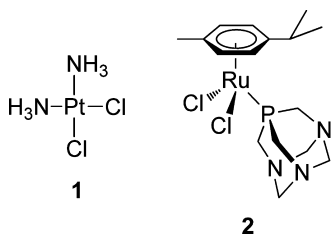


FIGURE 1. Complexes based on Pt (cisplatin; **1**) and Ru (Ru(*p*-cymene)(pta)Cl₂; **2**) demonstrate the utility of second and third row metals in biological applications.

The compatibility of metal ions with biology is forecasted by the variety of Lewis-basic sites found on biomolecules, ranging from the hydroxyl groups of sugars, the carboxylate, amine, and certain side-chain groups of amino acids, the *N*-heterocyclic rings of nucleotides and nucleic acids and other heterocycles, such as porphyrin rings, to name a few.¹ Bulk metal ions of Na, K, Mg, and Ca constitute as much as 1% of human body weight.² The remaining trace ions, most commonly of Fe, Ni, Cu, Mn, Zn, Co, Mo, and V, make up ~0.01% by weight; however, their importance in a number of processes cannot be overstated.²

Nature is limited to the use of bioavailable metal ions, which explains, in part, the wide number of first row metals found in exemplary biological processes. However, many biomolecules are well-suited to interact with rarer second and third row transition metals, which can elicit novel biological responses. A well-known example of a metal-based medicinal complex is cisplatin (**1**; Figure 1).³ The natural abundance, or lack thereof, of Pt explains its absence in natural systems. That said, its widespread application as an anticancer drug in the form of *cis*-Pt(NH₃)₂Cl₂ and analogous Pt(II) complexes is a testament to the relevance of late-metal ions in biology⁴ and has motivated numerous searches for new metalloanticancer drugs.⁵ Organometallic complexes represent a growing subset of potential anticancer drug molecules,⁶ with certain arene-Ru compounds showing high activity as antiproliferative agents, such as Ru(*p*-cymene)(pta)Cl₂ (**2**; Figure 1; pta = 1,3,5-triaza-phosphaadamantane).⁷ While biological applications of metal ions are certainly not limited to anticancer drug development, these hallmark Pt(II) and arene Ru investigations have motivated the use of coordination-driven self-assembly to form new biologically relevant materials due to the widespread use of both metal centers in the formation of supramolecular coordination complexes.

The use of metal–ligand bonding to drive the formation of metal–organic materials has been exploited in a number of synthetic strategies,⁸ furnishing a variety of related but

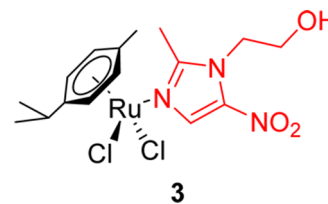


FIGURE 2. The first metal–arene compound evaluated for anticancer activity. The ligand in red is the antibiotic agent metronidazole.

structurally diverse species dominated by metal–organic frameworks (MOFs)⁹ and supramolecular coordination complexes (SCCs).¹⁰ Methods to form the latter are aptly described as *coordination-driven self-assembly*, reflecting that formation occurs from mixtures containing donor (metal) and acceptor (ligand) precursors, ideally generating unique discrete structures with metal–ligand bonding as the impetus.^{8,10}

The motivation for applying SCCs toward biological applications stems from a number of their inherent properties. First, the dimensions of a metallacycle or cage may be readily tuned without significant synthetic changes. Second, the specific metal ion used is versatile since coordination geometries are oftentimes predictable for a given element in a controllable oxidation state. Third, coordination-driven self-assembly allows for the incorporation of functional groups through pre- or post-self-assembly modifications.¹¹ Finally, the internal cavity of SCCs manifests host/guest capabilities which provide promise for sensing applications¹² as well as drug-delivery scaffolds,¹³ especially given the evidence that nanoscopic materials may show selective uptake in cancerous cells due to increased permeability.¹⁴

Ruthenium SCCs as Anticancer Agents

In 1992, Tocher and co-workers reported the first studies of an arene–ruthenium complex acting as an anticancer agent.¹⁵ The small drug molecule, Ru(*η*⁶-C₆H₆) (metronidazole)Cl₂ (**3**; Figure 2; metronidazole = 1-hydroxyethyl-2-methyl-5-nitroimidazole), incorporated the existing metronidazole antibiotic as the third ligand on a simple piano-stool Ru center. Interestingly, the selective cytotoxicity of complex **3** exceeded that of free metronidazole, illustrating that the inclusion of metal centers into a material can enhance the activity of existing drugs.

The latter strategy, utilizing host/guest chemistry to deliver a drug molecule, was described in an early biological application of SCCs by Therrien and co-workers¹⁶ which utilized the self-assembly of *p*-cymeneruthenium-based metal fragments with pyridyl donors, as pioneered in 1997 by Süss-Fink and co-workers.¹⁷ In this study, a trigonal prism was assembled by cofacially orienting two tritopic tripyridyl

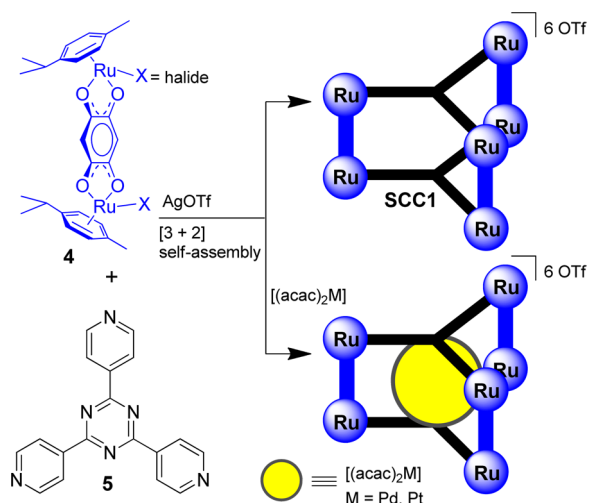


FIGURE 3. “Trojan Horse” SCC for anticancer drug delivery: a trigonal prismatic assembly with an internal cavity for host/guest chemistry.

ligands with three diruthenium molecular clips. By combining clip **4** with a 1,3,5-substituted triazine (**5**; Figure 3) in the presence of AgOTf, a [3 + 2] self-assembly occurred with simultaneous anion exchange to furnish $[\text{Ru}_6(p\text{-}^i\text{PrC}_6\text{H}_4\text{Me})_6(\text{tpt})_2(\text{dobq})_3]^{6+}$ (SCC1; $\text{tpt} = 2,4,6\text{-tris(pyridin-4-yl)-1,3,5-triazine}$, $\text{dobq} = 2,5\text{-dioxido-1,4-benzoquinonato}$). The trigonal prism was capable of encapsulating $[(\text{acac})_2\text{M}]$ ($\text{M} = \text{Pd}$, Pt ; $\text{acac} = \text{acetylacetonato}$), and the anticancer activities of the host/guest ensembles were compared to the prism and free guest molecules. The IC_{50} values were determined using A2780 human ovarian cancer cells and revealed that SCC1 ($\text{IC}_{50} = 23 \mu\text{M}$) was less effective than both the Pt and Pd host/guest ensembles ($\text{IC}_{50} = 12$ and $1 \mu\text{M}$ respectively), whereas the free $[(\text{acac})_2\text{M}]$ species were inactive. These results were rationalized by the observation that both $[(\text{acac})_2\text{Pt}]$ and $[(\text{acac})_2\text{Pd}]$ are insoluble in water and can only undergo cell-uptake encapsulated by the more-soluble trigonal prism. Subsequent release from the prism allowed the now-active cytotoxic Pd and Pt species to act in addition to the Ru centers.

SCC1 was also subjected to reactivity studies to determine the effects of various biomolecules on the stability of Ru-based SCCs in biological environments.¹⁸ ESI-MS and NMR were used to investigate the action of amino acids, ascorbic acid, and glutathione on the cage. These studies revealed that certain amino acids, specifically arginine, histidine, and lysine, all caused disassembly of SCC1, while methionine had no effect. Ascorbic acid and glutathione were catalytically oxidized, noted as a possible origin of cytotoxicity. These tests show the importance of carefully investigating the interactions of SCCs with biomolecules due to the

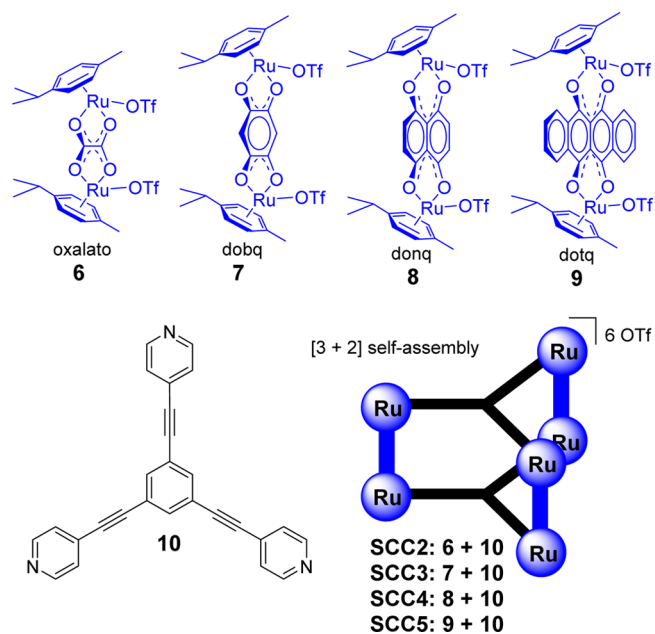


FIGURE 4. Trigonal prisms are obtained from the [3 + 2] assembly of a tritopic planar ligand with molecular clips.

TABLE 1. Cytotoxicities of Ru-Based Trigonal Prisms

	cell line IC_{50} values				
	SK-hep-1	HeLa	HCT-15	A-549	MDA-MB-231
SCC2	83.7	163.7	187.9	inact	inact
SCC4	3.8	9.2	4.1	3.4	7.6
cisplatin	6.3	10.5	5.6	2.4	2.7

potential for disassembly; mechanistic conclusions that invoke an intact SCC within an intercellular environment must be justified by stability experiments given the variety of decomposition vectors present.

Stang, Chi, and co-workers also assessed the activity of three-dimensional Ru-based SCCs, detailing the [3 + 2] self-assembly of four novel trigonal prisms (Figure 4).¹⁹ The ligand employed in these studies was 1,3,5-tris(pyridin-4-ylethynyl)benzene (**10**). In addition to a dobq -bridged molecular clip (**7**), three other diruthenium triflate salts were used, differing by their O,O_nO,O moieties, specifically oxalato (**6**),¹⁷ 5,8-dioxido-1,4-naphthoquinonato (donq ; **8**), and 5,11-dioxido-6,12-tetracenquinonato (dotq ; **9**) bridges. Anticancer activity was established using five cell lines, SK-hep-1 (liver), HeLa (cervix), HCT-15 (colon), A-549 (lung), and MDA-MB-231 (breast). While the prisms containing the dobq and dotq spacers were inactive across all cell lines, the oxalate and donq -based scaffolds were active, especially in the case of **4** (Table 1).

These activities suggest that there is no correlation between cytotoxicity and the size of the aromatic system of the

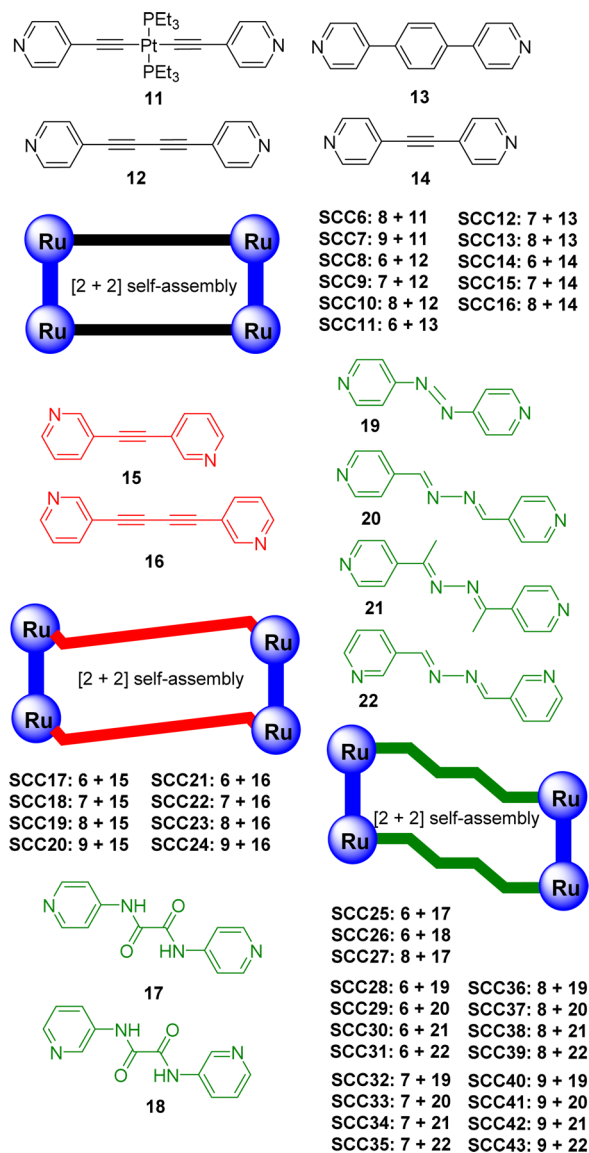


FIGURE 5. Molecular clips **6–9** undergo [2 + 2] assembly with linear donors **11–22** to furnish unique tetracationic metallacycles (SCC6–SCC43).

spacer ligand; the high activity of SCC4 was absent in its dotq-bridged counterpart. In addition, the dobq-based molecular clip, which was a component of the active SCC1, did not appear to manifest any anticancer properties in SCC3. These results highlight the importance of detailed mechanistic studies to isolate the factors associated with increased activity in order to guide future designs. For instance, a given ligand may provide the necessary dimensions for a particularly effective SCC, or may facilitate degradation to deliver active Ru-containing fragments, with the assembly acting as a prodrug.

While these pioneering studies indicate that trigonal prismatic cages may possess low IC_{50} values for particular combinations of donors and molecular clips, the most

TABLE 2. Cytotoxicities of Selected Active Rectangular SCCs

	cell line IC_{50} values/ μM (\pm)			
	SK-hep-1	HeLa	HCT-15	AGS
SCC6	5.36 (0.38)	9.40 (0.51)	9.83 (0.33)	2.65 (0.02)
SCC7	8.60 (0.65)	9.55 (0.87)	13.27 (0.03)	10.83 (0.30)
SCC8	51.08 (0.95)	14.91 (0.59)	11.40 (0.15)	9.61 (0.55)
SCC9	58.88 (0.08)	43.71 (2.08)	11.91 (0.10)	10.37 (0.69)
SCC10	15.45 (0.95)	20.48 (2.70)	15.23 (0.87)	11.65 (0.16)
SCC13	19.00 (4.99)		31.74 (5.49)	
SCC16	114.05 (2.69)		109.60	31.96 (2.25)
SCC19	6.97 (0.69)		7.46 (0.24)	
SCC20	29.53 (1.72)		39.45 (1.73)	
SCC21	66.19 (0.25)		53.66 (0.27)	
SCC22	63.58 (1.27)		57.05 (0.98)	
SCC23	9.60 (0.84)		10.66 (0.19)	
SCC24	16.32 (1.98)		17.68 (0.92)	
6	>200			
7	>200			
8	149.00 (2.01)			
9	>200			
cisplatin	12.38 (0.24)	76.85 (0.41)	8.38 (2.31)	>100
dox ^a	2.67 (0.24)	3.16 (0.04)	15.34 (0.58)	0.70 (0.16)

^adox = doxorubicin.

diverse subset of SCCs investigated for Ru-based anticancer activity are [2 + 2] self-assembly scaffolds. Early examples of [2 + 2] assemblies used in biological studies were given by Navarro, Barea, and co-workers²⁰ and Therrien and co-workers.²¹ The former report involved rigid dipyriddy-based ligands to form Ru metallacycles that underwent noncovalent binding with DNA and exhibited significantly different resistance factors to cisplatin. This result was taken as evidence for a different mode of action of the Ru SCCs versus Pt-based drugs.²⁰ The latter studies also used rigid dipyriddy ligands as well as pyrazine to bridge one of four Ru-clips. Biological assays revealed a range of toxicities for the eight metallacycles, ranging from 4 to 66 μM relative to the cisplatin control of 2 μM for A2780 ovarian cancer cells.²¹

Stang, Chi, and co-workers have reported a suite of [2 + 2] SCCs, each formed using molecular clips (**6–9**) and pyridyl-based donor ligands. The most straightforward of these assemblies incorporate the 4-pyridyl building blocks depicted in Figure 5.²² In vitro anticancer activities were assessed using four cancer cell lines, SK-hep-1 (liver), HeLa (cervical), HCT-15 (colon), and AGS (gastric). Of the 11 SCCs investigated, seven exhibited activity, as summarized in Table 2. The IC_{50} values of the corresponding clips were significantly higher, with only the donq clip showing measurable activity for SK-hep-1 cells.²³ The donq-based SCCs were particularly potent, with IC_{50} values oftentimes exceeding that of cisplatin, and on par with a second control drug, doxorubicin. The oxalato and dobq-containing species were relatively inactive in comparison. While the dotq ligand was present in SCC7, which had low IC_{50} values, this activity was

attributed not to the Ru-acceptor, but rather the Pt-containing donor ligand, **11**, which in combination with the donq molecular clip, **8**, gave by far the most active assembly, SCC6. In fact, this mixed-metal assembly had IC₅₀ values lower than those of cisplatin for all four cell lines. Some evidence for heightened activity resulting from longer donors was found, with assemblies using the long diethynyl spacer showing some efficacy; however, it is not immediately clear if this was due to length or other factors, such as the solubility differences between ethynyl moieties versus phenyl spacers.

The increased efficacy observed with extended, diethynyl spacers was reproduced using related 3-pyridyl-based donors, 1,2-di(pyridin-3-yl)ethyne, **15**, and 1,4-di(pyridin-3-yl)buta-1,3-diyne, **16**.²⁴ These two ligands were used with molecular clips **6–9** to form eight unique, distorted rectangular assemblies, SCC17–SCC24 (Figure 5). For the assemblies containing **15**, only the donq-based system exhibited low IC₅₀ values. The oxalato and dohq-based SCCs gave measurable cytotoxicities when combined with the longer diethynyl ligand, **16**. While the dotq-bridged SCC was slightly active with the shorter dipyridyl ligand (SCC20), the efficacy of the extended dotq assembly (SCC24) was much higher (Table 2). From these combined results, larger assemblies appeared to be more active than their shorter analogues, though the extent to which activity is directly affected by size versus indirect effects from size-dependent solubility differences and other factors warrants further investigation.

Related studies by Stang and Chi further expanded the library of biologically active SCCs. For example, by incorporating amide groups into the core of dipyridyl donors, **17** and **18**,²⁵ sites for hydrogen bonding were preserved and the presence of azo functionalities on donors **19–22** unlock potential photosensitization.²³ The assemblies formed from the combinations of **17–22** with **6–9** were investigated using five cell lines obtained from American Type Culture Collection for SCC25–SCC27: HeLa, HCT-15, and MDA-MB-231, SK-hep-1, A-549, with the latter two cell lines also used in assays with the sixteen azodipyridyl-based assemblies. SCC25 and SCC26, containing the oxalate bridged clip, were inactive, while rectangle SCC27, which employed the donq-bridged clip, possessed IC₅₀ values that were similar to those of cisplatin, with values (μM) of 4.2 ± 0.11 (SK-hep-1); 10.2 ± 0.21 (HeLa); 3.7 ± 0.10 (HCT-15); 3.2 ± 0.11 (A-549); 2.8 ± 0.03 (MDA-MB-231). Similar results were found for the azodipyridyl SCCs, with significant cytotoxicities found only for the donq-containing assemblies (SCC36–SCC39) with IC₅₀ values ranging from ~12 to 37 μM.

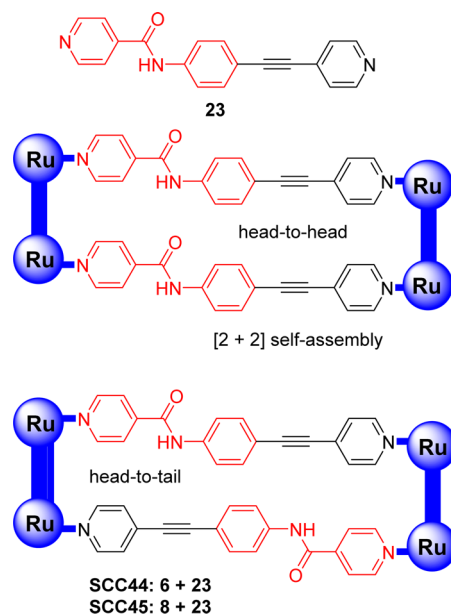


FIGURE 6. The use of asymmetric ligands gives rise to two possible isomers, head-to-head and head-to-tail.

TABLE 3. Cytotoxicities of Ru-Based Molecular Clips and Isomer Mixtures of SCCs Containing Asymmetric Donors

	cell line IC ₅₀ values/μM			
	A-549	Colo320	H1299	MCF7
1 (oxalato)	40.94	51.01	>100	>100
2 (donq)	18.05	12.95	>100	63.97
SCC44	38.86	>100	>100	80.91
SCC45	10.18	0.33	3.62	<0.1
cisplatin	>100	38.6	>100	>100

Another subset of [2 + 2] assemblies from Stang and Chi uses an asymmetric donor, *N*-(4-(pyridin-4-ylethynyl)phenyl)isonicotinamide (**23**).²⁶ The presence of two asymmetric ligands in a rectangular assembly results in two isomers based on their relative orientations (Figure 6). The head-to-head isomer (HTH) contains a mirror plane collinear with the ditopic donors that is absent in the head-to-tail isomer (HTT), being replaced by an inversion center. If no energetic preference exists, a statistical mixture is expected, which was the case when **23** was combined with clips **6** (oxalato) and **8** (donq). Once again, the rectangles formed using the donq-based clip had the lowest IC₅₀ values (Table 3). While the molecular clip precursors were moderately active for some cell lines, in all cases their corresponding [2 + 2] assemblies showed lower IC₅₀ values.

In addition to these cell viability studies, time-dependence of growth inhibition was investigated by preincubating the SCCs in a growth medium of 10% fetal bovine serum (FBS). The activity of SCC45 decreased to 50% of its full efficacy

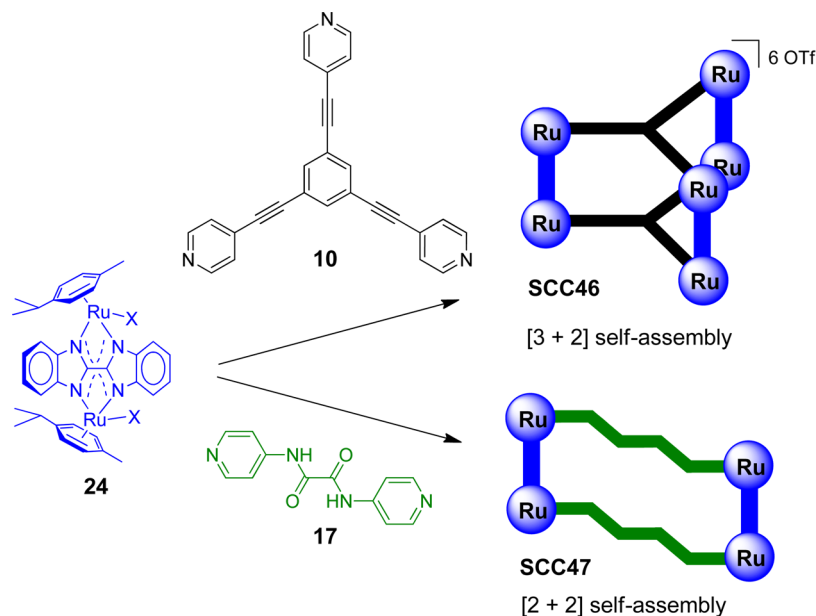


FIGURE 7. Molecular clip **24** can be used to form a trigonal prism or a rectangular metallacycle.

TABLE 4. Cytotoxicities of bis-Benzimidazole-Based SCCs

	cell line IC ₅₀ values/ μ M			
	A-549	Colo320	H1299	MCF7
24	>100	>100	>100	>100
SCC46	78.86	15.42	15.65	8.41
SCC47	13.94	>100	>100	80.91
cisplatin	38.6	>100	>100	>100

after 24 h, implicating the exogenous species present in FBS as responsible for the degradation.

Most recently, a new variant of the molecular clip was employed wherein the metal centers were bridged by a bis-benzimidazole ligand.²⁷ This clip was combined with tritopic ligand **10** and ditopic **17** to form a [3 + 2] prism and a [2 + 2] rectangular metallacycle, respectively (Figure 7). As summarized in Table 4, the IC₅₀ values of the prism, SCC46, were particularly low as compared to the free molecular clip, the rectangle, and cisplatin, with the exception of assay run with A-549 cells in which the rectangle was most effective.

These studies establish that Ru-based SCCs fulfill multiple roles in the development of new anticancer treatments. First, the ability of 3D prisms to act as hosts for anticancer drugs allows unfavorable properties associated with the free drug molecules to be circumvented, such as low solubility. Host/guest chemistry also provides a method to protect drug molecules from degradation en route to their targets by shielding the molecules from the cellular environment. In addition, the arene-Ru moieties of these SCCs impart inherent activity, with IC₅₀ values competitive with those determined for cisplatin and doxorubicin.

Metallosupramolecular Sensors

The internal cavities found in most 2D and 3D SCCs are well suited to act as receptor sites for small molecules. The careful selection of building blocks can impart a variety of useful properties, such as offering hydrogen bond donor and acceptor sites, tuning the hydrophobicity, spatial selection based on cavity size, etc. As such, the use of SCCs as sensors is a growing area of research.

Chi, Stang and co-workers described the synthesis and characterization of two arene-Ru-based SCCs formed via the [2 + 2] assembly of molecular clips **7** (dobq) and **9** (dotq) with the previously discussed diamide ligand, **17** (see Figure 8).²⁸ Absorption and emission titration studies revealed that SCC48 (**9** + **17**) exhibited minimal spectral changes when interacting with monoanionic species like halide anions or acetate (Figure 9). However, when rigid dianionic substrates were used, in this case the oxalate anion, noteworthy photophysical changes occurred. As oxalate exchange disruption is a marker for a number of diseases, it is an important oxyanion in biology.²⁹

The binding of oxalate was further probed by UV-vis titrations which indicated 1:1 stoichiometry. A Stern-Volmer constant of $5 \times 10^4 \text{ M}^{-1}$ was determined from photoluminescence titrations, indicative of a strong interaction between the SCC and oxalate. It was hypothesized that ground-state binding of oxalate to the amide receptor sites disrupted photoinduced electron transfer (PET) processes from the arene-Ru fragments which attenuated the quantum yield.

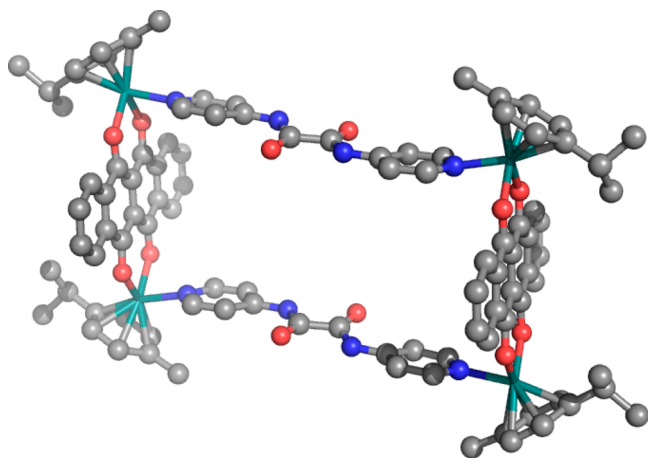


FIGURE 8. X-ray crystal structure of SCC48. Hydrogen atoms, solvent molecules, and counterions omitted for clarity. Atom (color): Ru (teal), N (blue), O (red), and C (gray).

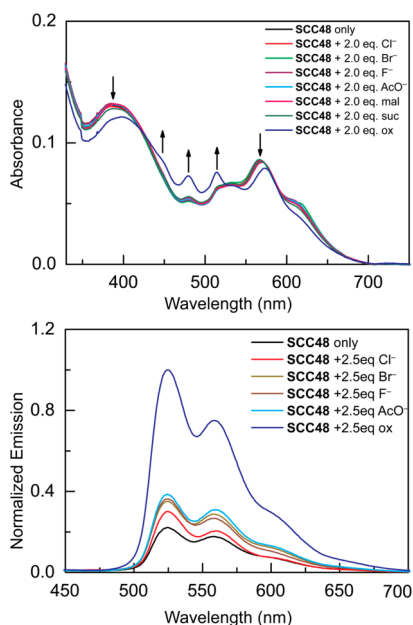


FIGURE 9. Absorption and emission responses of SCC48 to anionic analytes.

These results motivated further investigations using citrate and tartrate, two oxyanions that are relevant due to their role in a variety of biological processes.^{30,31} Both substrates induced emission enhancements, with Stern–Volmer constants of 1.4×10^5 and $1.8 \times 10^4 \text{ M}^{-1}$ for citrate and tartrate, respectively.

A follow-up study discussed the formation of so-called metalla-bowls which form via the [2 + 2] assembly of nonlinear ditopic donors with molecular clips (Figure 10).³² The spectral responses of SCC50 were selective for the multicarboxylate anions oxalate, tartrate, and citrate, with very little interaction with monoanions such as the halides, acetate, and benzoate (Figure 11).

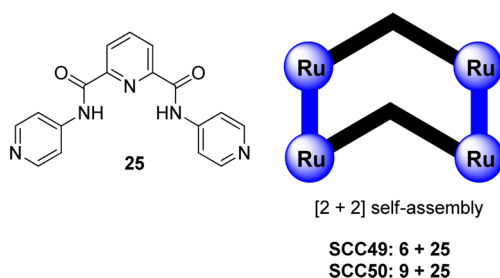


FIGURE 10. Nonlinear ditopic donors form wedge-shaped metalla-bowls when combined with molecular clips.

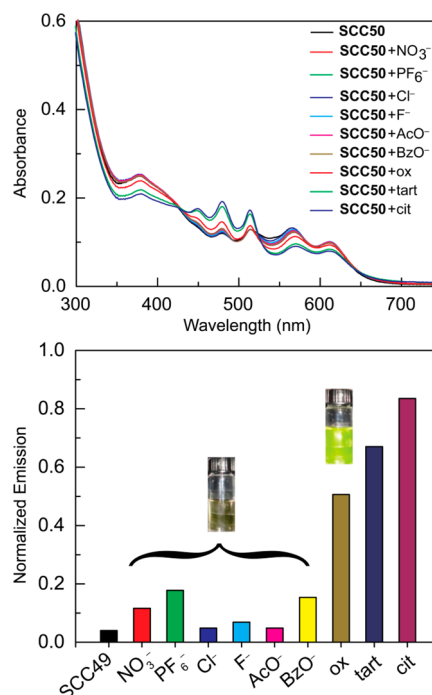


FIGURE 11. Spectral responses of SCC50 to the addition of anionic analytes.

Similar UV–vis and emission titration experiments were carried out with oxalate, furnishing a 1:1 binding model and Stern–Volmer constant of $1.5 \times 10^4 \text{ M}^{-1}$. Tartrate and citrate anions also gave strong interactions; Stern–Volmer kinetic analysis of SCC50 provided K_{sv} values of 1.9×10^4 and $2.7 \times 10^4 \text{ M}^{-1}$ for tartrate and citrate, respectively. These larger values relative to SCC48 indicate that the three-dimensional structures of arene-Ru-based assemblies play a role in their efficacies for binding substrates.

Metallacycle–DNA Interactions

Motivated in part by the interaction of zinc fingers with DNA and other biomolecules, Hannon and co-workers pioneered the self-assembly of bis(pyridylimine) ligands with metal ions to form metallosupramolecular cylinders.³³ The cylinders

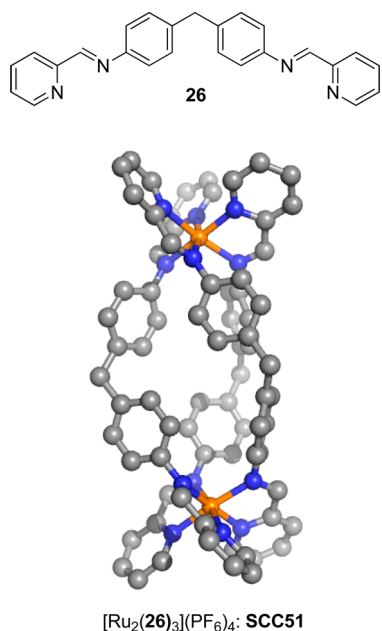


FIGURE 12. Structure M₂L₃ helicate SCC51. Solvent molecules, counterions, and hydrogen atoms omitted.

containing group 8 metals have been extensively studied and give rise to a number of DNA binding motifs. For instance, Fe-based cylinders can interact with the major groove of B-DNA, ultimately inducing coiling as characterized by circular and linear dichroism, microscopy and NMR experiments.³⁴ These same cylinders can recognize three-way DNA junctions, particularly highlighting the noteworthy π -stacking, intercalation, H-bonding, and other intermolecular interactions that can all occur simultaneously between a properly designed SCC and DNA constructs,³⁵ in some cases manifesting cytotoxicity without genotoxicity.³⁶ In keeping with the facile tunabilities associated with SCCs, impressive control over the helical chirality of these M₂L₃ constructs was illustrated by appending enantiopure arginine groups to the cylinders.³⁷ A second method for controlling chirality, established by Scott and co-workers, exploits ligands which give optically pure monomers. By tethering two such ligands into a ditopic building block, diastereomerically pure M₂L₃ assemblies are obtained.³⁸

In 2007, these experiments were expanded to Ru analogues upon the discovery of suitable synthetic conditions to furnish Ru₂(L)₃ triple helicates (SCC51, Figure 12). Like its Fe counterpart, the Ru cylinder also bound and induced coiling in DNA and exhibited cytotoxicities (IC₅₀ = 22, 53 μ M) marginally higher than those of cisplatin (4.9, 28 μ M) for HBL100 and T47D cell lines, respectively.³⁹ More recently, the Ru helicates were found to inhibit DNA transactions through in vitro PCR assays.⁴⁰ The extensive studies of

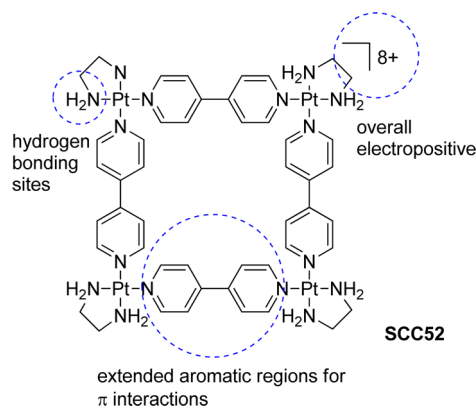


FIGURE 13. Supramolecular squares possess many attractive features for G-quadruplex stabilization.

Hannon and co-workers has also lead to the caveat that assays involving SCCs must be carefully conducted to avoid effects caused by incubation times or volumes, which can cause drastically different results for a single cell line, rendering single-point comparisons to cisplatin or other reference drugs potentially irrelevant.⁴¹

The stabilization of G-quadruplex motifs that form from the folding of G-rich sections of the single-stranded DNA telomere has been shown to inhibit the enzyme telomerase and the transcription activity of certain oncogenes. Since telomerase is active in $\sim 87\%$ of cancer cells, molecules which can stabilize G-quadruplex formation are potential anticancer agents. In 2008, Sleiman and co-workers recognized that a Pt-based SCC possessed many of the features predicted to afford strong G-quadruplex stabilization.⁴² Computational models predicted that [Pt(en)(4,4'-bipy)]₄(NO₃)₈ would have favorable binding to a 22-mer G-quadruplex structure (Figure 13). This model indicated that the ethylenediamine ligands were active in hydrogen bonding to phosphate oxygen atoms. Further stabilization was expected from interactions between the 4,4'-bpy rings and the guanine bases.

The binding was studied experimentally using a FRET melting assay which indicated a ΔT_m of 34.5 $^{\circ}$ C (the shift in the thermal denaturation temperature) with 0.75 μ M concentrations of SCC52. This stabilization slightly exceeded the values (27.5–33.8 $^{\circ}$ C) of known binders, which were studied at 1 μ M concentrations. An alternative measure of stabilization is the concentration required to achieve a ΔT_m of 20 $^{\circ}$ C, which was found to be 0.40 μ M for SCC52, again a very competitive value as compared to other known binders, which ranged from 0.38 to 0.70 μ M.⁴²

Studies of DNA stabilization by SCCs have since been extended to Ru-based assemblies. Vilar, Therrien and co-workers

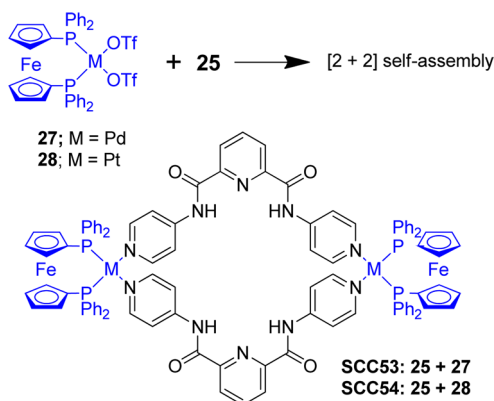


FIGURE 14. Heterobimetallic SCCs formed via the assembly of non-linear ditopic donors with square planar metal precursors.

have shown that tetragonal prisms formed from tetrapyrrolyl porphyrin and a *dobq*-based clip will bind to both telomeric and *c-myc* DNA, albeit with little selectivity between duplex and quadruplex strands.⁴³

SCCs containing Pd and Pt were also found to interact with supercoiled DNA based on studies by Chi, Stang, and co-workers.⁴⁴ The specific SCCs studied were heterobimetallic in nature due to the use of a ferrocenyl diphosphine ligand used to cap *cis* sites of the Pd and Pt precursors (**27** and **28**, respectively). [2 + 2] assembly of the metal precursors with the previously discussed nonlinear ditopic diamide dipyriddy ligand (**25**) furnished two rhomboid-like SCCs (Figure 14). Initial investigations of SCC53 and SCC54 with DNA used photophysical characterization. Both rhomboids displayed spectral changes upon titration of DNA into solution, with hypochromic shifts occurring throughout all absorption features. The corresponding K_{sv} values from emission titrations were $3.86 \times 10^3 \text{ M}^{-1}$ (SCC53) and $2.14 \times 10^3 \text{ M}^{-1}$ (SCC54), indicating significant fluorescence quenching in the presence of DNA.

The SCC/DNA interaction was further explored using gel electrophoresis which showed that both SCC53 and SCC54 were effective at unraveling supercoiled pUC19 DNA samples. While the Pd-based SCC was determined to have a higher binding constant, the electrophoresis studies indicated that the Pt-based rhomboid was better at unwinding the pUC19 sample, which was further corroborated by CD experiments in which a 50% decrease in the positive bands was observed commensurate with a blue-shift in wavelengths. Neither the donor nor acceptor precursors showed positive DNA unwinding.

Metallacycle–Protein Interactions

There has been growing interest in targeting proteins in the development of new drugs. Sava and co-workers put forth

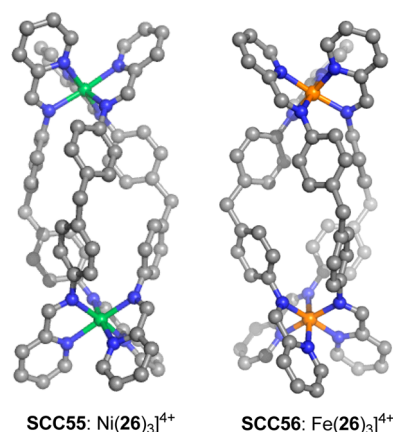


FIGURE 15. X-ray crystal structures of Ni (left) and Fe (right) SCCs. Hydrogen atoms, solvents, and counterions omitted for clarity.

the caveat that the dominant focus on DNA as a target for the development of new drugs and the exploration of mechanistic pathways may hinder the discovery of new anticancer agents.⁴⁵ To support this, they highlight the lack of understanding of DNA-adduct formation and efficacy of certain Pt-based anticancer drugs with specific tumor types.^{46,47} In addition, they reinforce the contradiction between the development of cisplatin resistance and the expression of DNA repair systems while pointing out that a correlation has been observed between the function of p35 mutant proteins and the activity of cisplatin.⁴⁸ A minireview by Casini and Reedijk⁴⁹ discusses examples of *in vitro* studies of existing Pt-based drugs provided clear evidence that these compounds are capable of interacting with proteins, sometimes affecting the mechanism of action.⁵⁰

A study by Qu and co-workers describes the use of triple-helical supramolecular cylinders which inhibit β -amyloid aggregation with implications for the treatment of Alzheimer's disease.⁵¹ These cylindrical SCCs are of the type used by Hannon and co-workers in their studies of DNA interactions (Figure 15).^{33,52}

The Fe-based SCC56 exhibited stronger inhibition over its Ni counterpart (SC55) using a fluorescence $A\beta$ -ECFP fusion assay. In addition to inhibiting aggregation, the cytotoxicity of both SCCs was evaluated using an MTT assay. When treated with $A\beta 1-40$, a decrease of 53% was observed, which could be prevented upon addition of the Ni or Fe SCC. When the complexes were used in the absence of $A\beta 1-40$, no effect was observed, implicating complex binding as an important mechanistic step. Further studies using rat models indicated that the compounds were effective in curing spatial memory defects induced by hyperhomocysteinemia. This work is the first example of aggregation inhibition

by SCCs and is a noteworthy proof-of-concept of the biological relevance that such compounds possess.

Conclusion

While the biological application of SCCs is still an emergent field of study, with the examples discussed here all based on publications only dating as far back as 2008, these pioneering results confirm supramolecular scaffolds have impressive relevance to a wide variety of biochemical and biomedical targets. Individual building blocks can be used to construct multifunctional SCCs, which in some cases can exhibit anticancer activity, act as selective sensors for biologically important analytes, and can interact with DNA and proteins. Due to the myriad of possible SCCs and the almost limitless modularity and tunability afforded without significant synthetic penalty, the biological applications of such species is expect to continue along this already promising path.

P.J.S. thanks the U.S. National Institutes of Health (NIH; Grant GM-057052) for financial support. K.W.C. gratefully acknowledges financial support from the World Class University (WCU) program (R33-2008-000-10003) and Priority Research Centers program (2009-0093818) through the National Research Foundation of Korea (NRF).

BIOGRAPHICAL INFORMATION

Timothy R. Cook received his B.A. degree from Boston University and his Ph.D. from the Massachusetts Institute of Technology. In 2010, he joined the Stang Group at Utah as a postdoc and later as an assistant research professor.

Vaishali Vajpayee obtained her Ph.D. from University of Rajasthan. In 2008, she joined the Chi Group as postdoc at Ulsan. In 2012, she moved to the University of Angers working with Prof. Marc Sallé.

Min Hyung Lee received B.S. and Ph.D. degrees from the Korea Advanced Institute of Science and Technology. He is currently an associate professor of chemistry in the University of Ulsan, Republic of Korea.

Peter J. Stang is a Distinguished Professor of Chemistry at Utah; a member of the U.S. National Academy of Sciences and the American Academy of Arts and Sciences; and the 2013 recipient of the ACS Priestley Medal.

Ki-Whan Chi received a Ph.D. degree from the University of Washington. He is currently a professor and the leader of BK21 and WCU projects in the Department of Chemistry, University of Ulsan.

FOOTNOTES

*To whom correspondence should be addressed.
The authors declare no competing financial interest.

REFERENCES

- Kraatz, H.-B.; Metzler-Nolte, N. *Concepts and models in bioinorganic chemistry*; Wiley-VCH: Weinheim, 2006.
- Bhattacharya, P. K. *Metal Ions in Biochemistry*; Alpha Science International Limited: Harrow, Middlesex, U.K., 2005.
- Sherman, S. E.; Lippard, S. J. Structural aspects of platinum anticancer drug interactions with DNA. *Chem. Rev.* **1987**, *87*, 1153–1181.
- Jung, Y.; Lippard, S. J. Direct Cellular Responses to Platinum-Induced DNA Damage. *Chem. Rev.* **2007**, *107*, 1387–1407.
- Kelland, L. The resurgence of platinum-based cancer chemotherapy. *Nat. Rev. Cancer* **2007**, *7*, 573–584.
- Jaouen, G., Ed. *Biorganometallics: Biomolecules, Labeling, Medicine*, John Wiley & Sons: Weinheim, Germany, 2006.
- Chatterjee, S.; Kundu, S.; Bhattacharya, A.; Hartinger, C.; Dyson, P. The ruthenium(II)–arene compound RAPTA-C induces apoptosis in EAC cells through mitochondrial and p53–JNK pathways. *J. Biol. Inorg. Chem.* **2008**, *13*, 1149–1155.
- Cook, T. R.; Zheng, Y.-R.; Stang, P. J. Metal–Organic Frameworks and Self-Assembled Supramolecular Coordination Complexes: Comparing and Contrasting the Design, Synthesis, and Functionality of Metal–Organic Materials. *Chem. Rev.* **2013**, *113*, 734–777.
- James, S. L. Metal-organic frameworks. *Chem. Soc. Rev.* **2003**, *32*, 276–288.
- Chakrabarty, R.; Mukherjee, P. S.; Stang, P. J. Supramolecular Coordination: Self-Assembly of Finite Two- and Three-Dimensional Ensembles. *Chem. Rev.* **2011**, *111*, 6810–6918.
- Wang, M.; Lan, W.-J.; Zheng, Y.-R.; Cook, T. R.; White, H. S.; Stang, P. J. Post-Self-Assembly Covalent Chemistry of Discrete Multicomponent Metallosupramolecular Hexagonal Prisms. *J. Am. Chem. Soc.* **2011**, *133*, 10752–10755.
- Wang, M.; Vajpayee, V.; Shanmugaraju, S.; Zheng, Y.-R.; Zhao, Z.; Kim, H.; Mukherjee, P. S.; Chi, K.-W.; Stang, P. J. Coordination-Driven Self-Assembly of M3L2 Trigonal Cages from Preorganized Metalloligands Incorporating Octahedral Metal Centers and Fluorescent Detection of Nitroaromatics. *Inorg. Chem.* **2011**, *50*, 1506–1512.
- Therrien, B. Drug Delivery by Water-Soluble Organometallic Cages. In *Chemistry of Nanococontainers*; Albrecht, M., Hahn, E., Eds.; Springer: Berlin Heidelberg, 2011; Vol. 319; pp 35–55.
- Matsumura, Y.; Maeda, H.; New, A. Concept for Macromolecular Therapeutics in Cancer Chemotherapy: Mechanism of Tumor-tropic Accumulation of Proteins and the Antitumor Agent Smancs. *Cancer Res.* **1986**, *46*, 6387–6392.
- Dale, L. D.; Tocher, J. H.; Dyson, T. M.; Edwards, D. I.; Tocher, D. A. Studies on DNA Damage and Induction of SOS Repair by Novel Multifunctional Bioreducible Compounds. II. A Metronidazole Adduct of a Ruthenium-arene Compound. *Anti-Cancer Drug Des.* **1992**, *7*, 3–14.
- Therrien, B.; Süß-Fink, G.; Govindaswamy, P.; Renfrew, A. K.; Dyson, P. J. The “Complex-in-a-Complex” Cations [(acac)2M⊂Ru6(p-IPrC6H4Me)6(tpbt)2(dhbq)3]6+: A Trojan Horse for Cancer Cells. *Angew. Chem., Int. Ed.* **2008**, *47*, 3773–3776.
- Yan, H.; Süß-Fink, G.; Neels, A.; Stoeckli-Evans, H. Mono-, di- and tetra-nuclear p-cymeneruthenium complexes containing oxalato ligands. *J. Chem. Soc., Dalton Trans.* **1997**, *0*, 4345–4350.
- Paul, L. E. H.; Therrien, B.; Furrer, J. Investigation of the Reactivity between a Ruthenium Hexacationic Prism and Biological Ligands. *Inorg. Chem.* **2011**, *51*, 1057–1067.
- Vajpayee, V.; Yang, Y. J.; Kang, S. C.; Kim, H.; Kim, I. S.; Wang, M.; Stang, P. J.; Chi, K.-W. Hexanuclear self-assembled arene-ruthenium nano-prismatic cages: potential anticancer agents. *Chem. Commun.* **2011**, *47*, 5184–5186.
- Linares, F. t.; Galindo, M. A.; Galli, S.; Romero, M. A.; Navarro, J. A. R.; Barea, E. Tetranuclear Coordination Assemblies Based on Half-Sandwich Ruthenium(II) Complexes: Noncovalent Binding to DNA and Cytotoxicity. *Inorg. Chem.* **2009**, *48*, 7413–7420.
- Mattsson, J.; Govindaswamy, P.; Renfrew, A. K.; Dyson, P. J.; Stěpnička, P.; Süß-Fink, G.; Therrien, B. Synthesis, Molecular Structure, and Anticancer Activity of Cationic Arene Ruthenium Metallarectangles. *Organometallics* **2009**, *28*, 4350–4357.
- Vajpayee, V.; Song, Y. H.; Yang, Y. J.; Kang, S. C.; Cook, T. R.; Kim, D. W.; Lah, M. S.; Kim, I. S.; Wang, M.; Stang, P. J.; Chi, K.-W. Self-Assembly of Cationic, Hetero- or Homonuclear Ruthenium(II) Macrocyclic Rectangles and Their Photophysical, Electrochemical, and Biological Studies. *Organometallics* **2011**, *30*, 6482–6489.
- Vajpayee, V.; Lee, S.; Kim, S.-H.; Kang, S. C.; Cook, T. R.; Kim, H.; Kim, D. W.; Verma, S.; Lah, M. S.; Kim, I. S.; Wang, M.; Stang, P. J.; Chi, K.-W. Self-assembled metalla-rectangles bearing azodipyridyl ligands: synthesis, characterization and antitumor activity. *Dalton Trans.* **2013**, *42*, 466–475.
- Vajpayee, V.; Song, Y. H.; Jung, Y. J.; Kang, S. C.; Kim, H.; Kim, I. S.; Wang, M.; Cook, T. R.; Stang, P. J.; Chi, K.-W. Coordination-driven self-assembly of ruthenium-based molecular-rectangles: Synthesis, characterization, photo-physical and anticancer potency studies. *Dalton Trans.* **2012**, *41*, 3046–3052.
- Vajpayee, V.; Song, Y. H.; Yang, Y. J.; Kang, S. C.; Kim, H.; Kim, I. S.; Wang, M.; Stang, P. J.; Chi, K.-W. Coordination-Driven Self-Assembly and Anticancer Activity of Molecular

- Rectangles Containing Octahedral Ruthenium Metal Centers. *Organometallics* **2011**, *30*, 3242–3245.
- 26 Mishra, A.; Jung, H.; Park, J. W.; Kim, H. K.; Kim, H.; Stang, P. J.; Chi, K.-W. Anticancer Activity of Self-Assembled Molecular Rectangles via Arene–Ruthenium Acceptors and a New Unsymmetrical Amide Ligand. *Organometallics* **2012**, *31*, 3519–3526.
- 27 Vajpayee, V.; Lee, S. m.; Park, J. W.; Dubey, A.; Kim, H.; Cook, T. R.; Stang, P. J.; Chi, K.-W. Growth Inhibitory Activity of a Bis-Benzimidazole-Bridged Arene Ruthenium Metalla-Rectangle and -Prism. *Organometallics* **2013**, *32*, 1563–1566.
- 28 Vajpayee, V.; Song, Y. H.; Lee, M. H.; Kim, H.; Wang, M.; Stang, P. J.; Chi, K.-W. Self-Assembled Arene–Ruthenium-Based Rectangles for the Selective Sensing of Multi-Carboxylate Anions. *Chem.—Eur. J.* **2011**, *17*, 7837–7844.
- 29 Morakot, N.; Rakrai, W.; Keawwangchai, S.; Kaewtong, C.; Wannoo, B. Design and synthesis of thiourea based receptor containing naphthalene as oxalate selective sensor. *J. Mol. Model.* **2010**, *16*, 129–136.
- 30 Pal, R.; Parker, D.; Costello, L. C. A europium luminescence assay of lactate and citrate in biological fluids. *Org. Biomol. Chem.* **2009**, *7*, 1525–1528.
- 31 Costello, L. C.; Franklin, R. B. Prostatic fluid electrolyte composition for the screening of prostate cancer: a potential solution to a major problem. *Prostate Cancer Prostatic Dis.* **2008**, *12*, 17–24.
- 32 Mishra, A.; Vajpayee, V.; Kim, H.; Lee, M. H.; Jung, H.; Wang, M.; Stang, P. J.; Chi, K.-W. Self-assembled metalla-bowls for selective sensing of multi-carboxylate anions. *Dalton Trans.* **2012**, *41*, 1195–1201.
- 33 Hannon, M. J.; Painting, C. L.; Jackson, A.; Hamblin, J.; Errington, W. An inexpensive approach to supramolecular architecture. *Chem. Commun.* **1997**, 1807–1808.
- 34 Hannon, M. J.; Moreno, V.; Prieto, M. J.; Moldrheim, E.; Sletten, E.; Meistermann, I.; Isaac, C. J.; Sanders, K. J.; Rodger, A. Intramolecular DNA Coiling Mediated by a Metallo-Supramolecular Cylinder. *Angew. Chem., Int. Ed.* **2001**, *40*, 879–884.
- 35 Oleksi, A.; Blanco, A. G.; Boer, R.; Usón, I.; Aymami, J.; Rodger, A.; Hannon, M. J.; Coll, M. Molecular Recognition of a Three-Way DNA Junction by a Metallo-supramolecular Helicate. *Angew. Chem., Int. Ed.* **2006**, *45*, 1227–1231.
- 36 Hotze, A. C. G.; Hodges, N. J.; Hayden, R. E.; Sanchez-Cano, C.; Paines, C.; Male, N.; Tse, M.-K.; Bunce, C. M.; Chipman, J. K.; Hannon, M. J. Supramolecular Iron Cylinder with Unprecedented DNA Binding Is a Potent Cytostatic and Apoptotic Agent without Exhibiting Genotoxicity. *Chem. Biol.* **2008**, *15*, 1258–1267.
- 37 Cardo, L.; Sadovnikova, V.; Phongsongpasuk, S.; Hodges, N. J.; Hannon, M. J. Arginine conjugates of metallo-supramolecular cylinders prescribe helicity and enhance DNA junction binding and cellular activity. *Chem. Commun.* **2011**, *47*, 6575–6577.
- 38 Howson, S. E.; Bolhuis, A.; Brabec, V.; Clarkson, G. J.; Malina, J.; Rodger, A.; Scott, P. Optically pure, water-stable metallo-helical 'flexicate' assemblies with antibiotic activity. *Nat. Chem.* **2012**, *4*, 31–36.
- 39 Pascu, G. I.; Hotze, A. C. G.; Sanchez-Cano, C.; Kariuki, B. M.; Hannon, M. J. Dinuclear Ruthenium(II) Triple-Stranded Helicates: Luminescent Supramolecular Cylinders That Bind and Coil DNA and Exhibit Activity against Cancer Cell Lines. *Angew. Chem., Int. Ed.* **2007**, *46*, 4374–4378.
- 40 Ducani, C.; Leczkowska, A.; Hodges, N. J.; Hannon, M. J. Noncovalent DNA-Binding Metallo-Supramolecular Cylinders Prevent DNA Transactions in vitro. *Angew. Chem., Int. Ed.* **2010**, *49*, 8942–8945.
- 41 Pope, A. J.; Bruce, C.; Kysela, B.; Hannon, M. J. Issues surrounding standard cytotoxicity testing for assessing activity of non-covalent DNA-binding metallo-drugs. *Dalton Trans.* **2010**, *39*, 2772–2774.
- 42 Kieltyka, R.; Englebienne, P.; Fakhoury, J.; Autexier, C.; Moitessier, N.; Sleiman, H. F. A Platinum Supramolecular Square as an Effective G-Quadruplex Binder and Telomerase Inhibitor. *J. Am. Chem. Soc.* **2008**, *130*, 10040–10041.
- 43 Barry, N. P. E.; Abd Karim, N. H.; Vilar, R.; Therrien, B. Interactions of ruthenium coordination cubes with DNA. *Dalton Trans.* **2009**, *0*, 10717–10719.
- 44 Mishra, A.; Ravikumar, S.; Hong, S. H.; Kim, H.; Vajpayee, V.; Lee, H.; Ahn, B.; Wang, M.; Stang, P. J.; Chi, K.-W. DNA Binding and Unwinding by Self-Assembled Supramolecular Heterobimetallics. *Organometallics* **2011**, *30*, 6343–6346.
- 45 Sava, G.; Jaouen, G.; Hillard, E. A.; Bergamo, A. Targeted therapy vs. DNA-adduct formation-guided design: thoughts about the future of metal-based anticancer drugs. *Dalton Trans.* **2012**, *41*, 8226–8234.
- 46 Sonpavde, G.; Sternberg, C. N. Satraplatin for the therapy of castration-resistant prostate cancer. *Future Oncol.* **2009**, *5*, 931–940.
- 47 Sanborn, R. Cisplatin Versus Carboplatin in NSCLC: Is There One "Best" Answer? *Curr. Treat. Options Oncol.* **2008**, *9*, 326–342.
- 48 Perrone, F.; Bossi, P.; Cortelazzi, B.; Locati, L.; Quattrone, P.; Pierotti, M. A.; Pilotti, S.; Licita, L. TP53 Mutations and Pathologic Complete Response to Neoadjuvant Cisplatin and Fluorouracil Chemotherapy in Resected Oral Cavity Squamous Cell Carcinoma. *J. Clin. Oncol.* **2010**, *28*, 761–766.
- 49 Casini, A.; Reedijk, J. Interactions of anticancer Pt compounds with proteins: an overlooked topic in medicinal inorganic chemistry? *Chem. Sci.* **2012**, *3*, 3135–3144.
- 50 Che, C.-M.; Siu, F.-M. Metal complexes in medicine with a focus on enzyme inhibition. *Curr. Opin. Chem. Biol.* **2010**, *14*, 255–261.
- 51 Yu, H.; Li, M.; Liu, G.; Geng, J.; Wang, J.; Ren, J.; Zhao, C.; Qu, X. Metallo-supramolecular complex targeting an [small alpha]/[small beta] discordant stretch of amyloid [small beta] peptide. *Chem. Sci.* **2012**, *3*, 3145–3153.
- 52 Kerckhoffs, J. M. C. A.; Peberdy, J. C.; Meistermann, I.; Childs, L. J.; Isaac, C. J.; Pearmund, C. R.; Reudegger, V.; Khalid, S.; Alcock, N. W.; Hannon, M. J.; Rodger, A. Enantiomeric resolution of supramolecular helicates with different surface topographies. *Dalton Trans.* **2007**, 734–742.